Brazilian Journal of Medical and Biological Research (2014) 47(12): 1029-1035, http://dx.doi.org/10.1590/1414-431X20144058
ISSN 1414-431X

Stability of *XIST* repression in relation to genomic imprinting following global genome demethylation in a human cell line

E.S.S. de Araújo[1,2], L.R. Vasques[1], R. Stabellini[1,2], A.C.V. Krepischi[1,2] and L.V. Pereira[1]

[1]Departamento de Genética e Biologia Evolutiva, Instituto de Biociências, Universidade de São Paulo, São Paulo, SP, Brasil
[2]Centro Internacional de Pesquisa, A.C. Camargo Cancer Center, São Paulo, SP, Brasil

Abstract

DNA methylation is essential in X chromosome inactivation and genomic imprinting, maintaining repression of *XIST* in the active X chromosome and monoallelic repression of imprinted genes. Disruption of the DNA methyltransferase genes *DNMT1* and *DNMT3B* in the HCT116 cell line (DKO cells) leads to global DNA hypomethylation and biallelic expression of the imprinted gene *IGF2* but does not lead to reactivation of *XIST* expression, suggesting that *XIST* repression is due to a more stable epigenetic mark than imprinting. To test this hypothesis, we induced acute hypomethylation in HCT116 cells by 5-aza-2′-deoxycytidine (5-aza-CdR) treatment (HCT116-5-aza-CdR) and compared that to DKO cells, evaluating DNA methylation by microarray and monitoring the expression of *XIST* and imprinted genes *IGF2*, *H19*, and *PEG10*. Whereas imprinted genes showed biallelic expression in HCT116-5-aza-CdR and DKO cells, the *XIST* locus was hypomethylated and weakly expressed only under acute hypomethylation conditions, indicating the importance of *XIST* repression in the active X to cell survival. Given that DNMT3A is the only active DNMT in DKO cells, it may be responsible for ensuring the repression of *XIST* in those cells. Taken together, our data suggest that *XIST* repression is more tightly controlled than genomic imprinting and, at least in part, is due to DNMT3A.

Key words: *XIST*; Imprinted genes; DNA methylation; 5-aza-2′-deoxycytidine; Human cell line

Introduction

Two striking epigenetic phenomena in mammalians are X chromosome inactivation (XCI) and genomic imprinting. XCI triggers the transcriptional silencing of most genes in all but one X chromosome in females (1), while genomic imprinting is a process that leads to monoallelic gene expression based on parental origin (2). DNA methylation, a covalent modification catalyzed by DNA methyltransferases (DNMTs) (3), is a key player of XCI and genomic imprinting. This and other epigenetic marks, such as histone modifications (4), are responsible for gene silencing in the inactive X chromosome and maintenance of *XIST* repression in the active X chromosome (5-8), and the monoallelic repression of imprinted genes is ensured by DNA methylation at either imprinting center regions (ICRs) or other cytosine-phosphate-guanine (CpG) controlling regions (9-12).

In the human male cancer cell line HCT116, disruption of the *DNMT1* and *DNMT3B* genes leads to global DNA hypomethylation and biallelic expression of the imprinted gene *IGF2* (13). In contrast, *XIST* repression is maintained when there is a decrease in DNMT1 and DNMT3B activity (14), suggesting that *XIST* repression is more tightly controlled than the allele-specific expression of imprinted genes. It has been shown that ectopic expression of *XIST* leads to inactivation of the transgene-containing autosome in male human cells (15). Thus, expression of *XIST* in a 46,XY cell may be detrimental, since it might silence the only X chromosome present in the cell. Therefore, lack of *XIST* expression in the DKO cell line could be due to selection during the relatively long process of knocking out the *DNMT1* and *DNMT3B* genes in HCT116 cells.

With the aim to test this hypothesis, we acutely induced DNA hypomethylation in parental HCT116 cells using 5-aza-2′-deoxycytidine (5-aza-CdR) and investigated the DNA methylation profile of the *XIST* locus and all imprinted genes described so far, as well as the expression of *XIST* and the three imprinted genes *IGF2*, *H19*, and *PEG10*.

Correspondence: L.V. Pereira: <lpereira@usp.br>

Received May 7, 2014. Accepted August 27, 2014. First published online October 17, 2014.

Material and Methods

Cell culture

The parental and double-knockout of *DNMT1* and *DNMT3B* (DKO) HCT116 cell lines were kindly provided by Drs. B. Vogelstein and K. Schuebel (13). Cells were cultured in McCoy media supplemented with 10% fetal calf serum and penicillin-streptomycin (Invitrogen, USA) at 37°C and 5% CO_2. Cells at the mid-log phase in 100-mm culture dishes were supplemented with fresh media containing 0.5 to 10 μM 5-aza-CdR in order to obtain the concentration that causes DNA hypomethylation similar to that seen in DKO. Fresh media with 5-aza-CdR was added every 24 h for 96 h, after which DNA and RNA were immediately extracted. The cell culture state was monitored visually throughout the treatments (Supplementary Figure S1).

Analysis of global methylation after 5-aza-CdR treatment

Genomic DNA (1 μg) was extracted with a FlexiGene DNA kit (Qiagen, Germany) and digested by 1 unit of *Msp*I or *Hpa*II (FastDigest, Fermentas, Germany) at 37°C overnight and resolved on 1% agarose gel. The intensity of non-digested (ND) or digested DNA bands was quantified by the ImageJ software (National Institutes of Health, USA). The percentage of Global DNA methylation was estimated as follows: % Methylation = (*Hpa*II – *Msp*I) ·100%/ND.

Genome-wide DNA methylation profile

A total of 1 μg of genomic DNA extracted from HCT116 and HCT116 cells treated with 10 μM 5-aza-CdR was bisulfite-converted using an EZ DNA methylation kit (Zymo Research, USA). The bisulfite-modified DNA samples were hybridized onto Infinium HumanMethylation450K BeadChip (Illumina, USA) following the manufacturer's instructions. The level of DNA methylation of each CpG was measured in β-values ranging from 0 to 1 [β = intensity of the methylated allele (M)/intensity of the unmethylated allele (U) + intensity of M + 100] using the GenomeStudio methylation module software (Illumina). DNA methylation data from the DKO cell line using the same platform (Infinium HumanMethylation450K BeadChip, Illumina) were retrieved from Gene Expression Omnibus (http://www.ncbi.nlm.nih.gov/geo/; accession number GSE29290, sample GSM815139).

The CpG probes related to imprinted genes, X chromosome, and *XIST* were retrieved from full data of the 450K microarrays and used for methylation analysis. Only probes with detection values of P≤0.01 and β-values for all samples were used for subsequent analysis. The list of human imprinted genes was built based on the Catalogue of Imprinted Genes (http://igc.otago.ac.nz) and Geneimprinting (www.geneimprint.com/) databases (Supplementary Table S1). For statistical analysis, we used the Kruskal-Wallis test at P≤0.05 and Dunn's multiple comparison test for *post hoc* analysis; both were performed using the GraphPad PRISM statistics software package (USA).

Analysis of *XIST* expression

Real-time reverse transcriptase-polymerase chain reaction (real-time RT-PCR). Total RNA was extracted using RNeasy (Qiagen, Germany) and treated with DNase Turbo DNA-Free (Ambion, USA) to avoid DNA contamination. One to two micrograms of total DNase-treated RNA were reverse transcribed using the SuperScript III first-strand synthesis system (Invitrogen, USA), and the *XIST* RNA level was determined by real-time RT-PCR (7500FAST Sequence Detection System; Applied Biosystems, USA) using the probe *XIST* (ID Hs01079824_m1; Applied Biosystems). *XIST* expression was normalized with the expression of *YWAHZ* [forward (F): TCCTTTGCTTGCATCCCA; reverse (R): AAGGCAGACAATGACAGACCA], described as a stable reference in the HCT116 cell line exposed to 5-aza-CdR (16). RNA fold expression was determined as previously described by Livak and Schmittgen (17). Two technical replicates of each reaction were performed.

RNA fluorescence in situ hybridization (RNA FISH). HCT116 cells were cultured and treated with 10 μM 5-aza-CdR for 96 h on Lab-Tek coverslips (Nunc, USA), and was followed by the modified RNA FISH protocol that was performed similar to that described by Chaumeil et al. (18). The *XIST* probe used is a 2.5 kb *XIST* cDNA containing exons 2, 3, 4, and 5, and was provided by Dr. Huntington

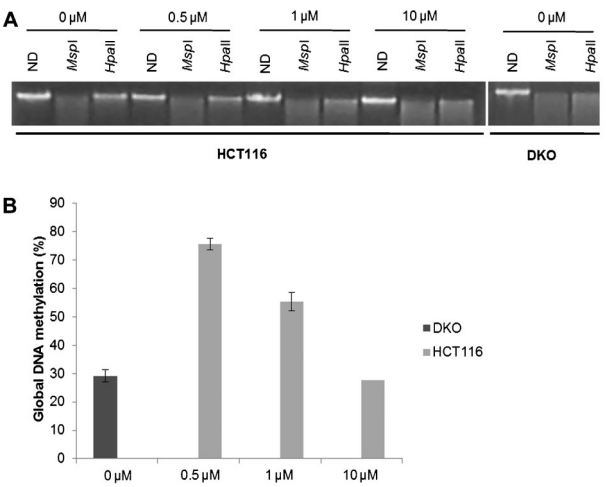

Figure 1. Global DNA methylation analysis. *A*, One percent agarose gel staining with ethidium bromide showing non-digested DNA (ND) and DNA digested with *Msp*I or *Hpa*II, which is an isoschizomer of *Msp*I methylation sensitive enzyme, at different media concentrations of 5-aza-2′-deoxycytidine (5-aza-CdR; 0, 0.5, 1.0, and 10 μM). *B*, Percentage of DNA methylation of each 5-aza-CdR treatment condition and DKO cells in relation to basal methylation of the HCT116 cell line (data from 2 different assays).

Willard (Case Western University, Cleveland, OH, USA). A total of 100 nuclei were analyzed.

Analysis of imprinted genes

Single nucleotide polymorphism (SNP) selection. Based on the National Center for Biotechnology Information (USA) dbSNP BUILD 129 (http://www.ncbi.nlm.nih.gov/SNP), we selected three imprinted genes that are expressed in human colorectal tumor, encompassing 13 SNPs located in coding regions (Supplementary Table S2). Primers for *IGF2* (F: 5′-CCTAGTCGTGGCTCTCCATC-3′; R: 5′-TTAAAGACAAAACCCAAGCATG-3′) and *H19* (F: 5′-AGCCCAACATCAAAGACACC-3′; R: 5′-AATGGAATGCTTGAAGGCTG-3′) were designed using Primer-Blast (http://www.ncbi.nlm.nih.gov/tools/primer-blast/); *PEG10* primers were described in Kim et al. (19).

Genotyping and analysis of allele-specific gene expression. DNA from HCT116 cells was extracted using a FlexiGene DNA kit (Qiagen). An aliquot of 100 ng of DNA was used as a template for PCR amplification of the region encompassing each SNP, in order to select the informative ones.

Synthesis of cDNA from HCT116, HCT116 5-aza-CdR-treated and DKO cells was performed as described above and used as templates for PCR amplification of the region encompassing each SNP. To control for DNA contamination, cDNA synthesis was performed in the presence or absence of reverse transcriptase. PCR products were resolved by 6% polyacrylamide gel electrophoresis and visualized by silver staining. Sequencing was carried out using the BigDye Terminator v3.1 cycle sequencing kit (Applied Biosystems), and analyzed by an ABI PrismH 3100 genetic analyzer, following the manufacturer's instructions (Applied Biosystems). At least two independent replicates were performed for each SNP.

Results

With the purpose of reaching the DNA methylation level similar to that achieved in DKO cells, we exposed HCT116 cells to increasing concentrations of 5-aza-CdR. We determined that 10 μM 5-aza-CdR for 96 h showed levels of hypomethylation comparable to those in DKO cells (Figure 1).

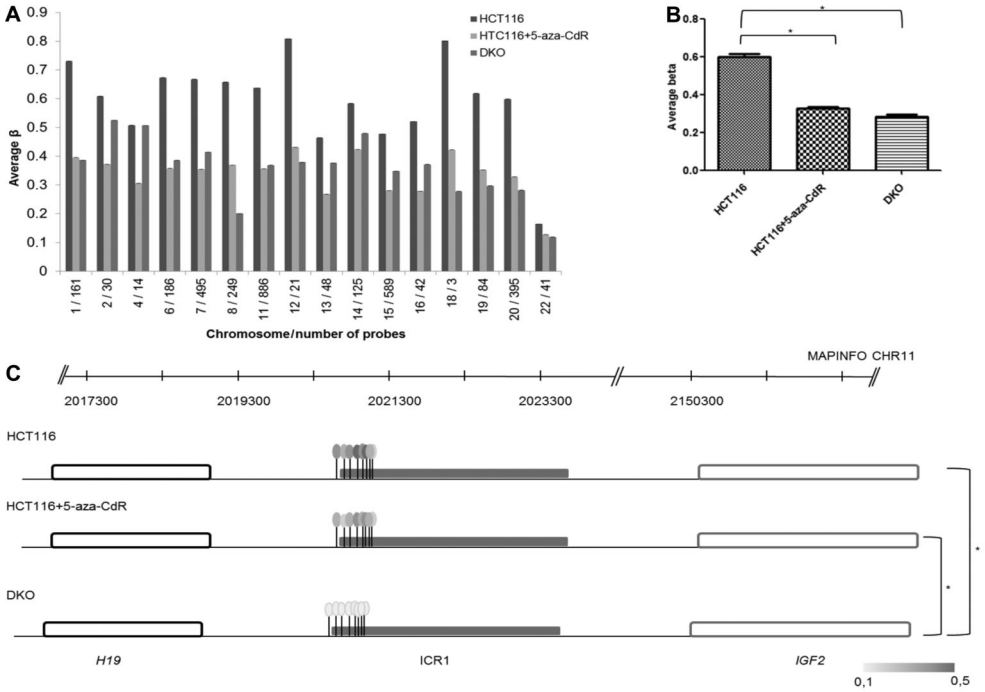

Figure 2. DNA methylation profile of CpGs (cytosine-phosphate-guanine) related to imprinted genes. *A*, The graph shows the DNA methylation level of CpG sites related to imprinted genes covered in the 450K platform, arranged per chromosome (β values average ranging from 0 to 1, unmethylated and fully methylated, respectively). Chromosomes 2, 4, and 8 presented methylation levels after 5-aza-CdR treatment different from DNMTs disruption (DKO cells; $P<0.0001$). *B*, Global DNA methylation level of all imprinted genes analyzed in the different cell lines. DKO and 5-aza-2′-deoxycytidine (5-aza-CdR)-treated cells exhibited statistically significant demethylation compared to HCT116 cells. *C*, Schematic view of the ICR1, the imprinting center of *IGF2* and *H19* genes, and the range of DNA methylation level of 8 CpGs sites (ovals) analyzed in this region (cg00237904, cg06765785, cg25821896, cg25574978, cg18454954, cg25579157, cg02886509 and cg02657360). The color-ratio bar at the bottom indicates the methylation level. DKO cells DNA methylation profile was retrieved from Gene Expression Omnibus: GSE29290, sample GSM815139. *$P<0.05$, Kruskal-Wallis test with Dunn's multiple comparison *post hoc* test.

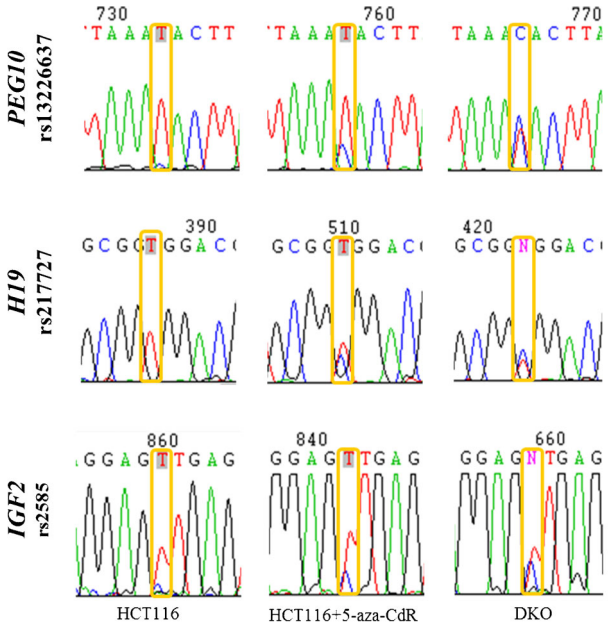

Figure 3. Expression pattern of the selected imprinted genes in the HCT116 cell line after 5-aza-2′-deoxycytidine (5-aza-CdR) treatment. Electropherograms of cDNA sequences of *PEG10*, *H19* and *IGF2* genes show the biallelic expression. Symbols of genes and corresponding single nucleotide polymorphism (SNP) ID are indicated at the side. SNP positions are highlighted in yellow.

DNA methylation patterns of all known imprinted human genes were investigated using the 450K platform, where 3369 CpGs sites associated with them were queried. HCT116 5-aza-CdR-treated cells exhibited a statistically significant decrease in methylation levels of these sites compared to untreated cells (Supplementary Table S2 and Figure 2A and B). Likewise, DKO cells showed a hypomethylated pattern at imprinted genes, equivalent to HCT116 5-aza-CdR-treated cells (Figure 2A and B). However, the ICR of *IGF2* and *H19* covered by eight probes (cg00237904, cg06765785, cg25821896, cg25574978, cg18454954, cg25579157, cg02886509, and cg02657360) showed a methylation pattern not significantly different between 5-aza-CdR-treated HCT116 cells and their untreated counterparts, but significantly different from DKO (Figure 2C). It is worth noting that the decrease in DNA methylation produced by 5-aza-CdR treatment or DNMT disruption is not similar among the chromosomes. At chromosomes 2 and 4, the 5-aza-CdR treatment leads to a DNA hypomethylation level not reached by DNMT disruption ($P<0.0001$). Conversely, chromosome 8 is less methylated in the DKO cells than in the 5-aza-CdR-treated HCT116 cells ($P<0.0001$).

To evaluate the expression pattern of the 3 selected imprinted genes (*IGF2*, *H19*, and *PEG10*), the HCT116 cell line was genotyped, and at least one informative SNP was identified in the expressed sequences of each gene (Supplementary Table S3). These imprinted genes showed monoallelic expression in HCT116 cells, but biallelic expression after 5-aza-CdR treatment, even under methylation levels not statistically different at ICR1 (Figures 3 and 2C).

XIST expression was evaluated by real-time RT-PCR. While HCT116 did not have detectable expression of *XIST*, 5-aza-CdR-treated HCT116 cells exhibited *XIST* expression, albeit approximately 25 times lower than female fibroblasts (Figure 4A). These data are consistent with RNA FISH analysis (Figure 4B), in which a *XIST* cloud was detected in only 2 of 100 analyzed nuclei from 5-aza-CdR-treated HCT116 cells. Despite the low *XIST* expression, 5-aza-CdR-treated HCT116 cells exhibited hypomethylation of the *XIST* locus (Figure 4C and Supplementary Table S4). In contrast, DKO cells do not show significantly different hypomethylation at the *XIST* locus compared to HCT116 cells, and they sustained *XIST* repression (Figure 4C). Additionally, the DNA methylation profile of the X chromosome was analyzed using the 450K platform, and a total of 10,966 CpGs sites investigated showed that 5-aza-CdR-treated cells were significantly less methylated than DKO cells in that chromosome (Figure 4D and Supplementary Table S5).

Discussion

Our aim was to verify if *XIST* repression is a more stable epigenetic mark than genomic imprinting under two different DNA hypomethylation conditions: a long-term loss of DNMT1 and DNMT3B activity (DKO cell line) and an acute loss of DNMT activity (HCT116-5-aza-CdR). While HCT116-5-aza-CdR cells showed patterns of decreased methylation at CpGs associated with *XIST* and imprinted genes, DKO cells exhibited hypomethylation only in imprinted genes. Consistent with this result, *XIST* is repressed in DKO cells and is weakly expressed in HCT116-5-aza-CdR; the imprinted genes *PEG10*, *IGF2*, and *H19* were biallelically expressed in both methylation-deficient cell lines.

The presence of *XIST* expression from the only X chromosome in the 5-aza-CdR-treated HCT116 cell line was previously reported by our group (14). Here, we extended this analysis showing that *XIST* was activated in only a few HCT116-5-aza-CdR cells, despite the *XIST* gene being hypomethylated. These findings may indicate that other epigenetic marks, such as histone modifications, are repressing *XIST* in this short-term assay (20). However, hypomethylated HCT116 cells in culture for long periods (DKO cells) showed DNA methylation levels at the *XIST* locus similar to untreated HCT116 cells, suggesting that DNMTs other than DNMT1 and DNMT3B might be responsible for *XIST* repression in DKO cells. Accordingly, there is evidence that Dnmt3a is responsible for both inactivation and maintenance of *Xist* repression

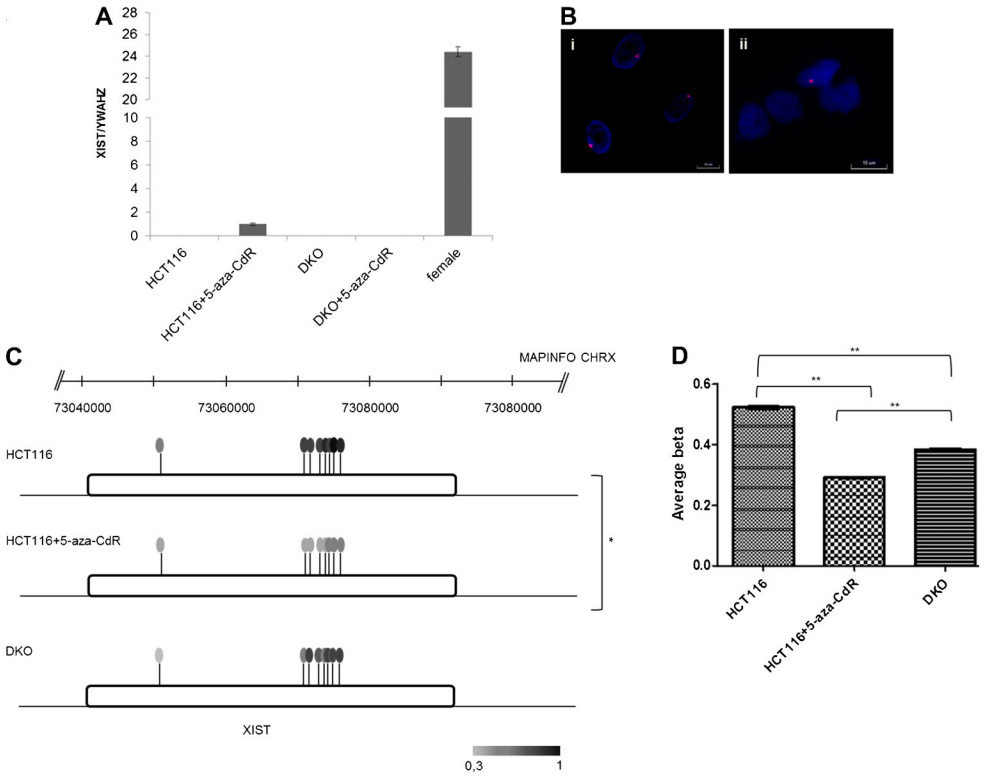

Figure 4. *XIST* expression. *A*, Relative expression levels of XIST RNA in HCT116 and a female cell line. The expression of *YWAHZ* was used as a reference. *B*, XIST RNA FISH in female cell line (*i*) and male HCT116 cell line treated with 10 μM 5-aza-CdR (5-aza-2′-deoxycytidine) for 96 h (*ii*). Nuclei were counterstained with DAPI (blue) and XIST RNA signals are red. The scale bar corresponds to 10 μm. *C*, *XIST* DNA methylation pattern by 8 CpGs (cytosine-phosphate-guanine) sites of 450K platform (cg15319295, cg12653510, cg05533223, cg117117280, cg20698282, cg17513789, cg02644889, and cg17279685). The color-ratio bar at the bottom indicates the methylation level. *D*, DNA methylation level of CpG sites related to X chromosome covered in the 450K platform; **P<0.0001, Kruskal-Wallis test with Dunn's multiple comparison *post hoc* test.

in murine ES cells and that it may help to keep global DNA methylation (21-23). Therefore, the absence of *XIST* expression in DKO cells might be due to the presence of DNMT3A.

In contrast, despite the importance of DNMT3A for the establishment of genomic imprinting during gametogenesis (24), this enzyme is not sufficient to keep monoallelic expression of imprinted genes, since DKO cells showed hypomethylation at imprinted genes and loss of imprinting (LOI). Whereas *XIST* expression and the consequent XCI could lead to the death of male cells, LOI may provide an advantage during cell proliferation, because it is a common feature in many types of cancer (25). Supporting this idea, biallelic expression of the imprinted genes *PEG10*, *IGF2*, and *H19* in the HCT116 cell line treated with 5-aza-CdR is also seen in DKO cells, even without any significant decrease in methylation of ICR1. Additionally, there is widespread hypomethylation in several CpG sites related to imprinted genes in DKO cells and in HCT116 after 5-aza-CdR exposure; thus, it is possible that other imprinted genes also show biallelic expression in HCT116 hypomethylated cells.

Therefore, our data suggest that *XIST* repression is more tightly controlled than the allele-specific expression of imprinted genes in a long-term loss of global DNA methylation. It is not known whether there is specific machinery for *XIST* repression or whether there is only cell selection against *XIST*-expressing cells; however, the control of *XIST* expression is more important for cell survival than the control of genomic imprinting. Nonetheless, our data indicate that DNMT3A might be responsible for *XIST* silencing in DKO cells, since DNA methylation levels are increased at the *XIST* locus in these cells, despite the absence of any other known active DNA methyltransferase. It is interesting to note that chromosomes 2, 4, and X are more methylated in DKO cells compared to 5-aza-CdR-treated HCT116 cells, suggesting that DNMT3A is involved in the repression of other genes in those chromosomes that may be important for long-term cell survival in culture.

Additionally, 5-aza-CdR treatment induces other effects than DNA hypomethylation. This drug is able to reduce the levels of G9A protein, decreasing H3K9me2, and resulting in gene activation (26). Also, 5-aza-CdR exposure can lead

to activation of the DNA damage response pathway, allowing pRb pocket protein degradation and a decrease in repressive posttranslational histone modifications (27). Thus, these additional effects of 5-aza-CdR can contribute to divergences in gene expression compared with DKO cells.

Finally, it is important to mention that these phenomena can occur in different ways in normal cells. Cancer cells have epigenomes very different from normal cells (28), making them susceptible to modifying agents of epigenetic marks, as demonstrated in several studies (29-33). Additional analyses will be important for comparing the maintenance of epigenetic controls associated with XCI and genomic imprinting in normal and transformed human cells.

Supplementary Material

Click here to view [pdf].

Acknowledgments

We gratefully acknowledge our colleagues Joana C.M. de Mello, Ana Maria Fraga, Simone A. Fonseca, Gustavo R. Fernandes, and Giovana C. Pirolla for their assistance. Research supported by FAPESP (#2008/07370-0).

References

1. Lyon MF. Gene action in the X-chromosome of the mouse (*Mus musculus* L.). *Nature* 1961; 190: 372-373, doi: 10.1038/190372a0.
2. Ferguson-Smith AC. Genomic imprinting: the emergence of an epigenetic paradigm. *Nat Rev Genet* 2011; 12: 565-575, doi: 10.1038/nrg3032.
3. Goll MG, Bestor TH. Eukaryotic cytosine methyltransferases. *Annu Rev Biochem* 2005; 74: 481-514, doi: 10.1146/annurev.biochem.74.010904.153721.
4. Escamilla-Del-Arenal M, da Rocha ST, Heard E. Evolutionary diversity and developmental regulation of X-chromosome inactivation. *Hum Genet* 2011; 130: 307-327, doi: 10.1007/s00439-011-1029-2.
5. Hendrich BD, Brown CJ, Willard HF. Evolutionary conservation of possible functional domains of the human and murine *XIST* genes. *Hum Mol Genet* 1993; 2: 663-672, doi: 10.1093/hmg/2.6.663.
6. Norris DP, Patel D, Kay GF, Penny GD, Brockdorff N, Sheardown SA, et al. Evidence that random and imprinted Xist expression is controlled by preemptive methylation. *Cell* 1994; 77: 41-51, doi: 10.1016/0092-8674(94)90233-X.
7. Panning B, Jaenisch R. DNA hypomethylation can activate Xist expression and silence X-linked genes. *Genes Dev* 1996; 10: 1991-2002, doi: 10.1101/gad.10.16.1991.
8. Tinker AV, Brown CJ. Induction of XIST expression from the human active X chromosome in mouse/human somatic cell hybrids by DNA demethylation. *Nucleic Acids Res* 1998; 26: 2935-2940, doi: 10.1093/nar/26.12.2935.
9. Fitzpatrick GV, Soloway PD, Higgins MJ. Regional loss of imprinting and growth deficiency in mice with a targeted deletion of KvDMR1. *Nat Genet* 2002; 32: 426-431, doi: 10.1038/ng988.
10. Stoger R, Kubicka P, Liu CG, Kafri T, Razin A, Cedar H, et al. Maternal-specific methylation of the imprinted mouse Igf2r locus identifies the expressed locus as carrying the imprinting signal. *Cell* 1993; 73: 61-71, doi: 10.1016/0092-8674(93)90160-R.
11. Thorvaldsen JL, Duran KL, Bartolomei MS. Deletion of the H19 differentially methylated domain results in loss of imprinted expression of H19 and Igf2. *Genes Dev* 1998; 12: 3693-3702, doi: 10.1101/gad.12.23.3693.
12. Williamson CM, Turner MD, Ball ST, Nottingham WT, Glenister P, Fray M, et al. Identification of an imprinting control region affecting the expression of all transcripts in the Gnas cluster. *Nat Genet* 2006; 38: 350-355, doi: 10.1038/ng1731.
13. Rhee I, Bachman KE, Park BH, Jair KW, Yen RW, Schuebel KE, et al. DNMT1 and DNMT3b cooperate to silence genes in human cancer cells. *Nature* 2002; 416: 552-556, doi: 10.1038/416552a.
14. Vasques LR, Stabellini R, Xue F, Tian XC, Soukoyan M, Pereira LV. XIST repression in the absence of DNMT1 and DNMT3B. *DNA Res* 2005; 12: 373-378, doi: 10.1093/dnares/dsi013.
15. Hall LL, Byron M, Sakai K, Carrel L, Willard HF, Lawrence JB. An ectopic human XIST gene can induce chromosome inactivation in postdifferentiation human HT-1080 cells. *Proc Natl Acad Sci U S A* 2002; 99: 8677-8682, doi: 10.1073/pnas.132468999.
16. Chua SL, See Too WC, Khoo BY, Few LL. UBC and YWHAZ as suitable reference genes for accurate normalisation of gene expression using MCF7, HCT116 and HepG2 cell lines. *Cytotechnology* 2011; 63: 645-654, doi: 10.1007/s10616-011-9383-4.
17. Livak KJ, Schmittgen TD. Analysis of relative gene expression data using real-time quantitative PCR and the 2(-Delta Delta C(T)) Method. *Methods* 2001; 25: 402-408, doi: 10.1006/meth.2001.1262.
18. Chaumeil J, Le Baccon P, Wutz A, Heard E. A novel role for Xist RNA in the formation of a repressive nuclear compartment into which genes are recruited when silenced. *Genes Dev* 2006; 20: 2223-2237, doi: 10.1101/gad.380906.
19. Kim KP, Thurston A, Mummery C, Ward-van Oostwaard D, Priddle H, Allegrucci C, et al. Gene-specific vulnerability to imprinting variability in human embryonic stem cell lines. *Genome Res* 2007; 17: 1731-1742, doi: 10.1101/gr.6609207.
20. Morey C, Avner P. The demoiselle of X-inactivation: 50 years old and as trendy and mesmerising as ever. *PLoS Genet* 2011; 7: e1002212, doi: 10.1371/journal.pgen.1002212.
21. Chen T, Ueda Y, Dodge JE, Wang Z, Li E. Establishment and maintenance of genomic methylation patterns in mouse embryonic stem cells by Dnmt3a and Dnmt3b. *Mol Cell Biol* 2003; 23: 5594-5605, doi: 10.1128/MCB.23.16.5594-5605.2003.
22. Jones PA, Liang G. Rethinking how DNA methylation patterns are maintained. *Nat Rev Genet* 2009; 10: 805-811, doi: 10.1038/nrg2651.

23. Okano M, Bell DW, Haber DA, Li E. DNA methyltransferases Dnmt3a and Dnmt3b are essential for de novo methylation and mammalian development. *Cell* 1999; 99: 247-257, doi: 10.1016/S0092-8674(00)81656-6.
24. Kaneda M, Okano M, Hata K, Sado T, Tsujimoto N, Li E, et al. Essential role for de novo DNA methyltransferase Dnmt3a in paternal and maternal imprinting. *Nature* 2004; 429: 900-903, doi: 10.1038/nature02633.
25. Uribe-Lewis S, Woodfine K, Stojic L, Murrell A. Molecular mechanisms of genomic imprinting and clinical implications for cancer. *Expert Rev Mol Med* 2011; 13: e2, doi: 10.1017/S1462399410001717.
26. Wozniak RJ, Klimecki WT, Lau SS, Feinstein Y, Futscher BW. 5-Aza-2′-deoxycytidine-mediated reductions in G9A histone methyltransferase and histone H3 K9 di-methylation levels are linked to tumor suppressor gene reactivation. *Oncogene* 2007; 26: 77-90, doi: 10.1038/sj.onc.1209763.
27. Zheng Z, Li L, Liu X, Wang D, Tu B, Wang L, et al. 5-Aza-2′-deoxycytidine reactivates gene expression via degradation of pRb pocket proteins. *FASEB J* 2012; 26: 449-459, doi: 10.1096/fj.11-190025.
28. Baylin SB, Jones PA. A decade of exploring the cancer epigenome - biological and translational implications. *Nat Rev Cancer* 2011; 11: 726-734, doi: 10.1038/nrc3130.
29. Atadja P, Gao L, Kwon P, Trogani N, Walker H, Hsu M, et al. Selective growth inhibition of tumor cells by a novel histone deacetylase inhibitor, NVP-LAQ824. *Cancer Res* 2004; 64: 689-695, doi: 10.1158/0008-5472.CAN-03-2043.
30. Bender CM, Pao MM, Jones PA. Inhibition of DNA methylation by 5-aza-2′-deoxycytidine suppresses the growth of human tumor cell lines. *Cancer Res* 1998; 58: 95-101.
31. Lee JH, Choy ML, Ngo L, Venta-Perez G, Marks PA. Role of checkpoint kinase 1 (Chk1) in the mechanisms of resistance to histone deacetylase inhibitors. *Proc Natl Acad Sci U S A* 2011; 108: 19629-19634, doi: 10.1073/pnas.1117544108.
32. Liang G, Gonzales FA, Jones PA, Orntoft TF, Thykjaer T. Analysis of gene induction in human fibroblasts and bladder cancer cells exposed to the methylation inhibitor 5-aza-2′-deoxycytidine. *Cancer Res* 2002; 62: 961-966.
33. Ungerstedt JS, Sowa Y, Xu WS, Shao Y, Dokmanovic M, Perez G, et al. Role of thioredoxin in the response of normal and transformed cells to histone deacetylase inhibitors. *Proc Natl Acad Sci U S A* 2005; 102: 673-678, doi: 10.1073/pnas.0408732102.